Journal of Renewable Materials

Tech Science Press

Value-Added Utilization of Agro-Waste Derived Oil Palm Ash in Epoxy Composites

Samsul Rizal[1], Fizree, H. M.[2], Chaturbhuj K. Saurabh[3], Deepu A. Gopakumar[2], N. A. Sri Aprilia[4], D. Hermawan[5], A. Banerjee[6], Fazita M. R. M[2], Haafiz M. K. M.[2] and Abdul Khalil H. P. S.[2,*]

[1]Department of Mechanical Engineering, Universitas Syiah Kuala, Banda Aceh, Indonesia.

[2]School of Industrial Technology, Universiti Sains Malaysia, Penang, Malaysia.

[3]Food Technology Division, Bhabha Atomic Research Centre, Trombay, Mumbai, India.

[4]Department of Chemical Engineering, Universitas Syiah Kuala, Banda Aceh, Indonesia.

[5]Department of Forestry, Kampus IPB, Darmaga, Bogor Agricultural University, Bogor, West Java, Indonesia.

[6]Department of Biotechnology and Microbiology, Tilak College of Science and Commerce, University of Mumbai, Mumbai, India.

[*]Corresponding Author: Abdul Khalil H. P. S. Email: akhalilhps@gmail.com.

Abstract: Oil palm ash (OPA) is an agro-industry waste and it has disposable problems. In the present study, an effort was made for value addition to OPA by incorporating it as a micro-filler in different concentration (0, 10, 20, 30, 40, and 50%) and sizes (100, 200, and 300 mesh size particles) in the epoxy matrix. Prepared micro OPA was having a crystallinity index of 65.4%, high inorganic elements, and smooth surface morphology. Fabricated composites had higher void content as compared to neat epoxy matrix. Mechanical properties of fabricated composites had a maximum value at 30% loading of 300 mesh-size filler due to its low void content and size as compared to filler of 100 and 200 mesh size. Further increase in the concentration of OPA filler after 30 wt% of loading leads to the agglomeration of OPA microparticles and thereby resulted in the reduction of mechanical characteristics such as tensile strength, tensile modulus, flexural strength and flexural modulus of the composites. However, elongation at break decreased with increase in filler content at all percentage. Thermal stability and char residue percentage of composite increased with the concentration of filler at all percentage. Surface morphology of composite showed that OPA incorporation lead towards its roughness and cracks were originated from the site of OPA embedded in the epoxy matrix. The 300 mesh-size particles were having the best effect on composite as compared to 100 and 200 mesh-size filler.

Keywords: Oil palm ash; micro filler; epoxy composite

1 Introduction

In tropical countries like South East Asia, oil palm has become one of the prominent economic crops. Malaysia, being the second largest global exporter of palm oil leads to a tremendous amount of generation of oil palm and waste associated with it. Waste biomass from oil palm industry includes oil palm trunk, oil palm fronds, empty fruit bunches, palm kernel shell, and mesocarp fiber which comprised of 18.09%, 58.05%, 8.97%, 5.45%, and 9.44% (all dry weight %), respectively [1]. These fibrous waste biomasses are often used as boiler fuel in palm mills for steam electricity generation [2]. After combustion in the steam boiler, about 5% (weight %) of ash called oil palm ash (OPA) is produced generating another type of solid waste [3]. Malaysia alone generates about 4 million tons of OPA annually. OPA is siliceous in nature and this has drawn the interest of researchers to look for its various potential applications such as cement

replacement material, adsorbent for the removal of zinc from aqueous solution, and flue gas desulphurization [4-6]. Still, most of the OPA generated ends up in landfill causing environmental problems.

Another approach for value addition to OPA is, used it as a filler in the matrix to form composites. Filler incorporation can reduce overall composite cost as well as provide specific performance benefits. Composite materials exhibit combined properties of their constituent components (including matrix and fillers) such display of properties is not possible by either ingredient in isolation. Filler effectively absorbs energy from polymer matrix under stress thus improving its mechanical properties. High inorganic content of filler such as silica enhances the thermal stability of composites. Biomass-based filler such as cellulose from bamboo, wood, flax, etc. are frequently used to improve the mechanical and barrier properties of composites [7-9]. The potential of OPA as a filler in composites had been studied by several researchers. The utilization of this solid waste as filler in polymer composites is very important, firstly as wastes are available abundantly at no cost; secondly, as the disposal of this waste poses an environmental problem.Mechanical, thermal, physical, and morphological properties of the composites upon the incorporation of OPA vary depending on its concentration [10] and size [11]. OPA incorporation in unsaturated polyester [12] and epoxy [13] resulted in improved tensile, flexural, and thermal properties of composites. Effect of micro-sized OPA in polymer concrete and nano-sized OPA in epoxy was investigated as a filler and both types of fillers significantly improved the properties of fabricated composites [13,14]. However, there is no report available on the utilization of OPA microparticle as a reinforcement in epoxy composite with exploration in different microparticle size and filler loading.In the present study, an attempt has been made to investigate the effect of different micro-sized OPA fillers in different loading percentage on various properties of epoxy-based composites.

2 Experimental

2.1 Preparation and Characterization of OPA as Micro Filler Material

OPA was obtained from United Palm Oil Mill, NibongTebal Penang, Malaysia. The precursor of OPA was a mixture of nut shells, fibers, and empty fruit bunches which were combusted at 300ºC in an incinerator. Obtained OPA was initially dried at 105°C for 24 hrs to remove moisture. Dried OPA was sieved with 60 mesh size sieve to remove impurity such as sands, pebbles, etc. Later OPA was first grounded by using MF 10 basic microfine grinder, IKA®, Germany. The rotor speed was set at 6500 rotation/min. Finally, OPA was sieved by 100, 200, and 300mesh size sieve. Obtained micro fillers were stored in a desiccator at 0% RH till further use. The density of OPA samples were measured at 22.8°C with a pressure of 19.477 psig by Digital Density meter Gas pycnometer AccuPyc 1330, USA. The surface area was determined from the adsorption isotherms using Brunauer-Emmett-Teller (BET) equation and Quantachrome Nova Win2© 1994-2002, Austria. The particle size of grounded OPA filler was assessed on a Malvern Zetasizer Nano Series (Netherlands) by dynamic light scattering measurements by means of a 532 nm laser.The chemical composition of the particles was monitored and recorded with the aid of the X-Ray Fluorescence (XRF) branded PANalytical model Axios MAX powered 4kW Dutch-made.

2.2 XRD Analysis of OPA

X-ray diffraction patterns of the micro OPA was obtained by using a Philips PW1050 X-pert diffractometer using Cu-Kα1 radiation operating at 40 kV and 25 Ma with $\lambda = 1.54$ Å. The diffractograms were scanned from 0° to 90° (2θ) in steps of 0.02° using a scanning rate of 0.5 °C/min. X-Ray diffractogram of OPA was carried out for determining the degree of crystalline or amorphous nature of the samples and crystallite size [15]. The diffractometer was controlled by a personal computer equipped with X-pert High Score puls Software.

2.3 Preparation and Characterization of Epoxy Based Micro Composites

The microstructured OPA of different sizes (100, 200, and 300 mesh size) was mixed with epoxy composites at five different concentrations (10, 20, 30, 40, and 50 wt.% of epoxy). For the development

of composite, a stainless steel mould with dimensions of 160 mm × 160 mm × 3 mm was used. Epoxy resin (D.E.R 331, Zarm Scientific & Supplies Sdn. Bhd., Malaysia) was mixed with 10% diluents (benzyl alcohol) to decrease the viscosity and then blended with OPA filler at room temperature for 30 minutes using a mechanical stirrer at 3000 rpm. Then 50 parts curing agent (polyamine hardener) in 100 parts epoxy by weight was added. The mixture was once again stirred for 10 minutes at 170 rpm. Later obtained mixture was degassed in a vacuum chamber for 15 minutes to remove bubbles. The blend was then cast into a mould and the composites were left to cure at 105°C for 1 hour in a hot press (Gotech Hot Press-Gt-7014; Taichung Industry Park, Taichung City, Taiwan) at 200 psi. Post curing was done in an oven at 105°C for 30 minutes. Composites density was measured by using ASTM-D1895, 1996 standard. For determination of voids content in composites ASTM-D2734, 1999 method was used. In the present work, physical properties of the prepared composites were measured by using an INSTRON 5582 universal testing machine, USA. Tensile test of the prepared composite was done in accordance with ASTM-D3039, 2000 specifications. The flexural analysis was carried out at room temperature through three-point bend testing as specified in ASTM-D790, 2003 standard. Izod notched impact testing was carried out using Geotech testing machine, Model GT-7045 MD (Taiwan). The Izod impact test samples with a dimension of 70 mm × 15 mm × 3 mm were cut by a circular saw and tested at ambient condition according to ASTM-D256, 2006a standards.

2.4 Morphology of OPA Filler and Composites

Morphology of raw and grounded OPA was investigated by using field emission scanning electron microscope (FESEM) (Leo Supra, 50 VP, Carl Ziess, SMT, Germany). 1 to 3 mg of samples were mounted onto FESEM holder using double-sided electrically conducting carbon adhesive tapes to prevent surface charge on the specimens when exposed to the electron beam. Prior to the morphological observation, sample surface was sputtered with 20 nm thick layer of gold using a Polaron Equipment Limited model E500 with the voltage set at 1.2 kV (10 mA) and a vacuum of 20 Pa for 10 min. The FESEM micrographs were obtained under conventional secondary electron imaging conditions with an acceleration voltage of 5 kV. The Izod impact fractured surface of micro-sized OPA filled epoxy composites was also investigated by using a scanning electron microscope.

2.5 Thermogravimetric Analysis (TGA)

A Perkin Elmer thermal gravimetric analyzer (TGA-6, USA) was used to investigate the thermal stability of the composites. The powder of composites and neat epoxy (about 4-5 mg) were heated from 30 to 800°C under nitrogen at a heating rate of 20 ^{o}C/min.

3 Results and Discussion

3.1 Physical and Chemical Properties of Micro Fillers

Fig. 1(A) shows the particle size distribution of micro fillers. Average diameter, density, and surface area of samples were summarized in Tab. 1. The 300 mesh size OPA exhibited the highest surface area which was 4.6198 m^2/g followed by 200 mesh and 100 mesh size with a value of 1.0778 m^2/g and 0.084 m^2/g, respectively. It was observed that particle size was inversely proportional to the surface area [16]. Fillers with the large surface area can have more interaction with the matrix resulting in a greater possibility of energy transfer from matrix to filler thus improving the mechanical properties of composites [17]. No significant change in the density of OPA samples was noted in the present study. The chemical composition analysis showed that the major components found in raw OPA were silicon dioxide (SiO_2), calcium oxide (CaO), and potassium oxide (K_2O) having 60.98%, 11.34%, and 8.25%, respectively. While various trace elements such as Ba, Br, Cl, Cr, Cu, Ni, Rb, S, Sm, Sr, Y, Zn, and Zr were present in OPA. Presence of SiO_2 and trace elements could possibly improve the thermal properties of OPA filled composites [18].

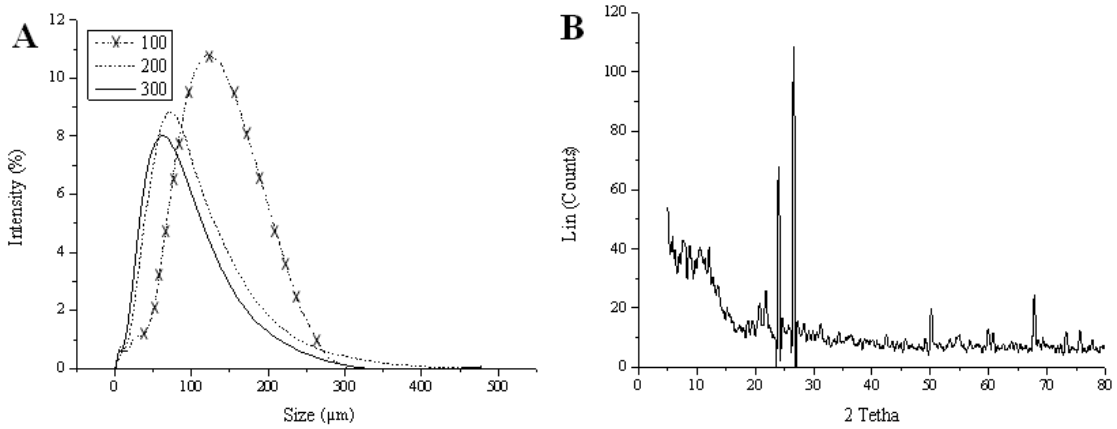

Figure 1: (A) Particle size distribution of micro OPA filler; (B) XRD spectroscopy of OPA ranging from 2θ (5°-80°)

Table 1: Particle size, density, and surface area of OPA

Size	Average diameter (μm)	Density (g/m^3)	Surface area (m^2/g)
100	138.64	2.622	0.084
200	72.15	2.64	1.0778
300	50.12	2.686	4.6198

3.2 Crystallinity Index

The crystallinity index (CI) of OPA was found to be 65.4%. OPA exhibited a higher degree of crystallinity, as evidenced by numbers of crystalline peaks in the diffractogram. Peaks at 24.02°, 26.52°, 50.20°, and 67.87° were significant and showed a crystalline form (Fig. 1(B)). An amorphous region was observed between 27° to 48° and this might be due to the presence of amorphous glassy material [19].

3.3 Surface Morphology of Micro Fillers

A morphological study of raw and grounded OPA had been performed under FESEM and presented in Figs. 2(A) and 2(B). Typically, raw OPA consist of irregular and angular shaped particles with spongy porous like structure with a sizable fraction showing cellular textures [20-22]. However, grounded OPA had micro-sized particles and crushed shape structures with no pores. Absence of pores in grounded fillers could be resulted in the good mechanical properties of the composites when compared to raw filler which has large pores.

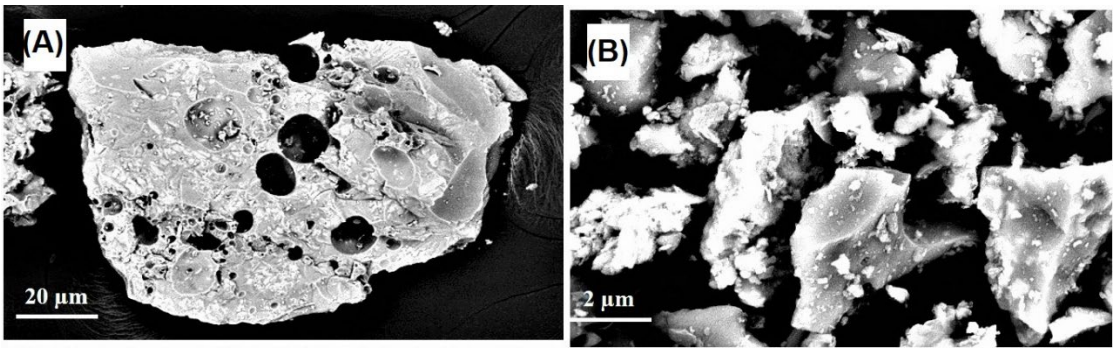

Figure 2: FESEM Micrograph of; (A) raw OPA (5k ×); (B) grounded OPA (500k ×)

3.4 Physical Properties of Micro Composites

Density and void content of micro-sized OPA filled epoxy composites were investigated to determine the effects of OPA filler size and loading concentration on physical properties of developed composites. Tab. 2 shows the theoretical and measured densities of microstructured OPA filled epoxy composites with different filler size and filler loading along with the void content percentage. Neat epoxy had an average theoretical and measured density of 1.12 g/cm^3 and 1.096 g/cm^3, respectively. OPA filler incorporation leads to an increase in densities of all types of composites. Measured density increased to 1.327 g/cm^3, 1.337 g/cm^3, and 1.349 g/cm^3 for 50% loading of 100, 200, and 300 mesh size filler, respectively. This increase in density of the composites was attributed to the incorporation of high-density micro OPA (Tab. 1) in the low-density epoxy matrix. Increase in density was inversely proportional to mesh size filler and directly proportional to filler percentage. Difference between measured and theoretical density was due to the presence of voids in the composites. Percentage of voids increased with increase in filler loading. Furthermore, it was also noticed that composites with smaller filler size (300 mesh) had less void than 200 and 100 mesh size filler loaded composites. Voids significantly affect the mechanical properties of composites. Higher void contents usually mean lower fatigue resistance, poor mechanical properties, greater susceptibility to water penetration and weathering resistance [23].

Table 2: Effect of size and concentration of micro OPA on density and void content of epoxy composites

Loading filler content (%)	Measured density (g/cm^3)	Theoretical density (g/cm^3)	Void content (%)
Neat	**1.096**	**1.112**	**1.378**
100 Mesh Size			
10	1.139	1.173	2.932
20	1.191	1.230	3.185
30	1.240	1.282	3.286
40	1.286	1.331	3.386
50	1.327	1.376	3.524
200 Mesh Size			
10	1.148	1.173	2.144
20	1.200	1.230	2.481
30	1.249	1.283	2.632
40	1.294	1.332	2.843
50	1.337	1.377	2.946
300 Mesh Size			
10	1.159	1.174	1.302
20	1.213	1.232	1.538
30	1.262	1.285	1.809
40	1.306	1.335	2.180
50	1.349	1.382	2.354

3.5 Mechanical Properties of Micro Composites

In order to determine the optimum particle size and filler loading in epoxy mechanical properties of composites were investigated (Fig. 3). Fig. 3(A) shows the effect of particle size and filler loading on the tensile strength of micro epoxy composites. At all loading percentage epoxy composites with 300 mesh size particles had higher tensile strength than 200 and 100 mesh size filler. All composites displayed a similar pattern of enhancement in tensile strength up to 30 wt% of filler loading. Further increase in filler concentration led to a reduction in tensile strength. The native composite had a tensile strength of 45.4 MPa and this increased to a value of 61.6 MPa for 30% filler of 300 mesh size and later strength reduced to a value of 52.3 MPa for 50% filler of the same size. The surface area is higher for smaller particles size; therefore better interfacial adhesion and load transfer between filler and polymer thus improved mechanical properties [24]. At higher filler concentration tensile strength decreased this was probably because of agglomeration of OPA additives thus causing premature failure [25]. Tensile modulus also followed the trend of tensile strength as shown in Fig. 3(B). Smaller the particle size higher was the tensile modulus. With an increase in all types of filler concentration tensile modulus increases until 30% of filler thereafter decrease in tensile modulus was demonstrated by composites. For 30 mesh size OPA, tensile modulus increased from 0.77 GPa to 1 GPa and then decreased respectively to a value of 0.86 GPa for 0%, 30%, and 50% filler loading. Elongation at break of composites is shown in Fig. 3(C). Neat epoxy demonstrated the highest elongation at break among all the studied samples with a value corresponding to 6.04%. However, elongation at break decreases with the filler sizes and at all loading percentage. The observed reduction in ductility of the composite with smaller particle sizes was due to an increase in deformation of rigid interfacial interaction between smaller fillers and matrix [26]. Reduction in elasticity with the increase in concentration was due to the filler aggregation which creates an area of stress concentrations that require less energy to propagate cracks [27]. Impact strength, flexural strength, and flexural modulus followed the trend of tensile strength and tensile modulus (Figs. 3(D), 3(E), and 3(F)). The 300 mesh particle size had the highest flexural strength, impact strength,and flexural modulus among all the investigated samples. All filler exhibited highest flexural and impact properties at 30% filler loading with further increase in micro OPA resulted in poor strength of the composites.

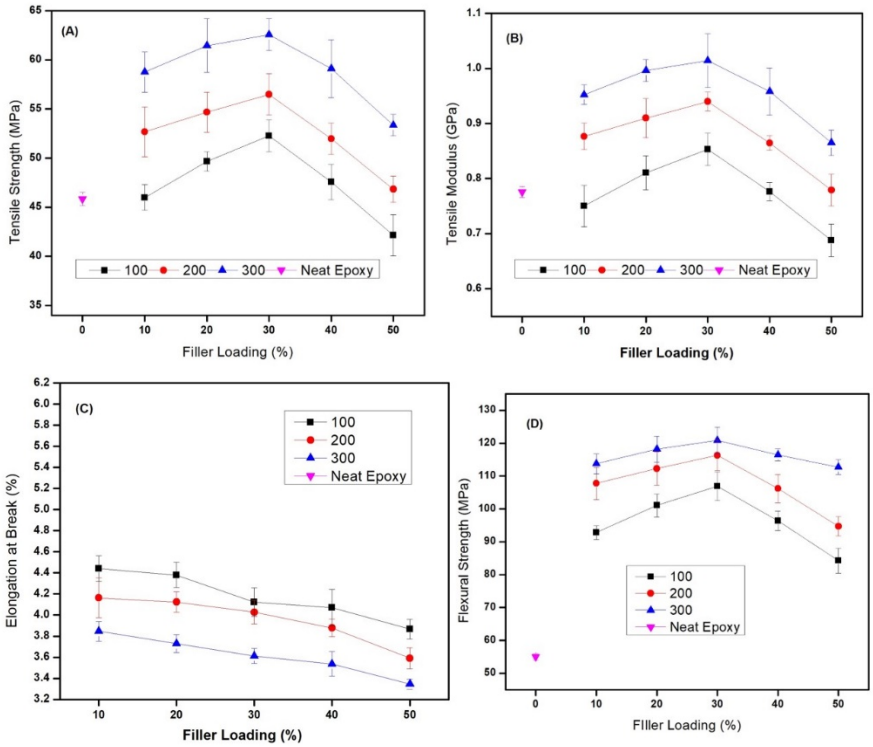

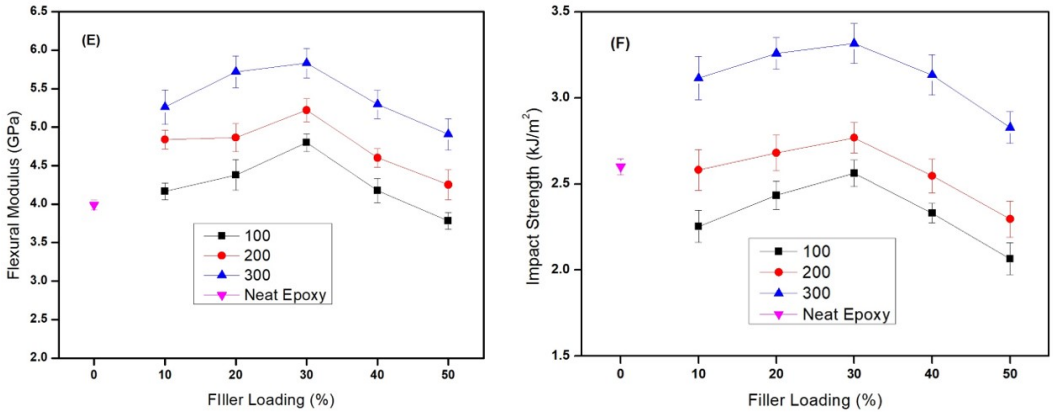

Figure 3: Effect of particle size and filler loading on (A) Tensile strength; (B) Tensile modulus; (C) Elongation at break; (D) Flexural strength; (E) Flexural modulus; (F) Impact strength

3.6 Thermogravimetric Analysis of Micro Composites

Tab. 3 shows the effect of particle size and filler loading on the thermal stability of microstructured OPA filled epoxy composites.Neat epoxy showed the lowest thermal stability and char residue among all the studied composites. The T_i, T_f, and T_{max} of neat epoxy were 323.1°C, 382.6°C, and 341.4°C, respectively. Observed thermal properties of composites were due to high SiO_2 contents in OPA (Section 3.1) and this provides better thermal stability, strength, hardness to composites [18]. Moreover, OPA also contains many inorganic elements (Section 3.1) beside SiO_2 that can withstand high temperatures [13]. Similar findings were reported by other research groups for composites containing various metal oxides which enhanced its thermal stability [28]. With the increase in filler percentage degradation temperature also increased for all mesh size OPA filled composites.

Table 3: Effect of particle size and filler loading on thermal properties of micro OPA filled epoxy composites

Composites		Degradation Temperature (°C)		Char Residue (%)	DTG peak Temperature (°C)
		T_i	T_f		T_{max}
Neat Epoxy		**323.1**	**382.6**	**5.95**	**351.4**
100	10	347.5	410	10.29	362.6
	20	351.5	413	12.66	366.6
	30	353.7	414	13.10	366.8
	40	354.9	414	15.45	367.0
	50	360.1	416	19.30	367.6
200	10	352.5	408	9.40	367.9
	20	359.3	413	11.29	369.8
	30	359.8	420	12.32	370.6
	40	359.9	425	14.00	370.9
	50	360.4	426	17.71	372.2
300	10	348.2	417	15.16	362.5
	20	352.5	420	21.19	372.2
	30	358.2	424	21.33	372.9
	40	359.9	426	24.47	373.9
	50	362.8	427	25.94	374.0

3.7 Fractured Surface Morphologies of Micro Composites

The Fractured surface of micro composites is presented in Fig. 4. Crack propagation was from bottom to top in all the investigated samples. It was observed that the fractured surface of neat epoxy was smooth with thin river lines parallel to the crack propagation direction, which indicates that the crack propagated rapidly, and little energy was absorbed during fracture [29] as shown in the Fig. 2(A), hence, the resistance to crack.

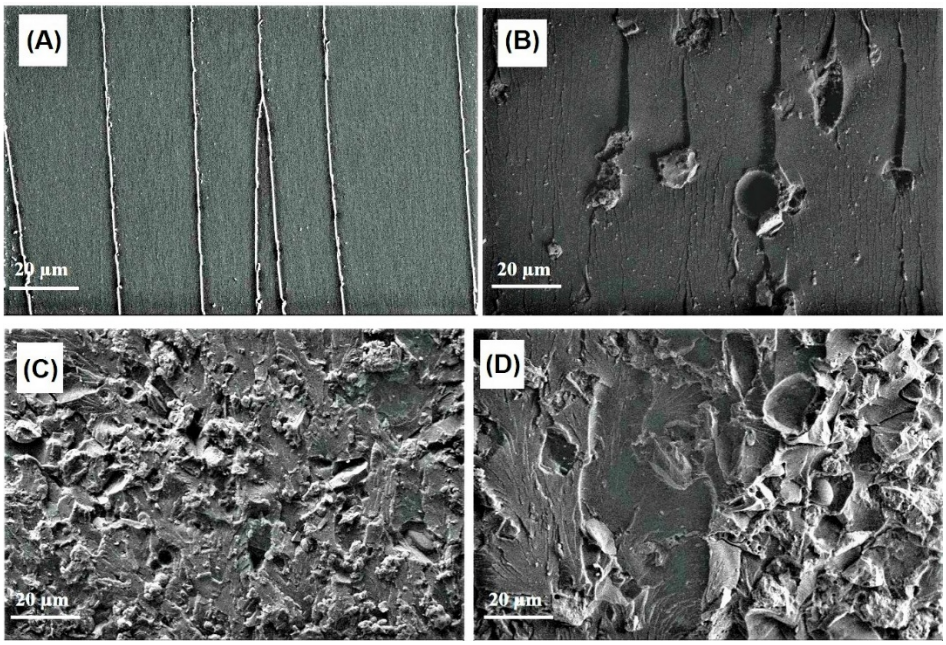

Figure 4: FESEM micrograph of (A) Fractured surface of neat epoxy; (B) Fractured surface of composite with 10% filler of 100 mesh size; (C) Fractured surface of composite with 20% filler of 100 mesh size (F) Fractured surface of composite with 10% filler of 100 mesh size; (D) Fractured surface of composite with 50% filler of 100 mesh size

Propagation was less and leads to brittle failure. Also, there were no voids present which could act as crack propagation sites. Micrograph of composites with 100 mesh size OPA revealed a clear contrast between the patterns of fracture and particles (Figs. 2(B) and 2(C)). Filler addition also leads to the roughness of the micro composites. Cracks were often originated from the site of OPA particles embedded in the epoxy (Fig. 2(C)). Increase in filler loading leads to the agglomeration of filler particles (white circle) in epoxy as observed in Fig. 2(D) and this causes the reduction in strength of composites. The agglomerated OPA would act as stress concentration site when applied stress and not the individual microparticles. This made the cracks penetrated through them hence initiate the failure [13]. A similar observation was also made in composites with 200 and 300 mesh size particles.

4 Conclusions

In this study, micro OPA was prepared and used as reinforcement for the fabrication of epoxy-based polymer composites. Micro fillers were obtained by grinding and sieving into 3 different particle sizes including 100, 200, and 300 mesh size having an average diameter of 138.64, 72.15, and 50.12 µm, respectively. OPA contained a high amount of silica and a crystallinity index of 65.4% with smooth surface morphology. It was further observed that tensile, flexural, and impact properties of composites demonstrated the highest value at 30% filler loading of 300 mesh size. Observed enhancement in properties was due to the energy transfer from matrix to filler under stress. With further increase in filler loading to 40% and above resulted in a decrease in all the above mention properties because of

agglomeration of micro OPA. However, elongation at break showed a consistent decrease with increase in loading percentage of filler. Thermogravimetric analysis of micro composites revealed that the incorporation of OPA improved the thermal stability of composites at all concentration. Char residue was also found lowest in neat epoxy as compared to all other samples. The observed improvement in thermal stability was due to the presence of high SiO_2 and various inorganic elements. Thus, the improvement in mechanical and thermal properties of micro OPA incorporated epoxy-based composites was demonstrated in the present study.

Acknowledgments: This work was financially supported by Ministry Research, Technology and Higher Education of Republic of Indonesia by World Class Professor (WCP), Programme scheme No T/46/D2.3/KK.04.05/2019. The authors would like to thank the collaboration between Department of Mechanical Engineering, Universitas Syiah Kuala, Bhabha Atomic Research Centre, Mumbai and School of Industrial Technology, Universiti Sains Malaysia, Penang, Malaysia that has made this work possible.

References

1. Foo, Y. N., Foong, K. Y., Basiron, Y., Sundram, K. (2011). A renewable future driven with malaysian palm oil-based green technology. *Journal of Oil Palm & the Environment, 2,* 1-7.
2. Aghamohammadi, N., Reginald, S. S., Shamiri, A., Zinatizadeh, A. A., Wong, L. P. et al. (2016). An investigation of sustainable power generation from oil palmbiomass: a case study in Sarawak. *Sustainability, 8(5),* 416.
3. Mazenan, P. N., Khalid, F. S., Shahidan, S., Shamsuddin, S. M. (2017). Review of palm oil fuel ash and ceramic waste in the production of concrete. *IOP Conference Series: Materials Science and Engineering, 271,* 012051.
4. Thomas, B. S. (2018). Green concrete partially comprised of rice husk ash as a supplementary cementitious material-A comprehensive review. *Renewable and Sustainable Energy Reviews, 82(3),* 3913-3923.
5. Mondal, P., George, S. (2015). A review on adsorbents used for defluoridation of drinking water. *Reviews in Environmental Science and Bio/Technology, 14(2),* 195-210.
6. Thomas, B. S., Kumar, S., Arel, H. S. (2017). Sustainable concrete containing palm oil fuel ash as a supplementary cementitious material-A review. *Renewable and Sustainable Energy Reviews, 80,* 550-561.
7. Rizal, S., Abdul Khalil, H. P. S., Bhat, I. U. H., Huzni, S., Thalib, S. et al. (2018). Recent advancement in physico-mechanical and thermal studies of bamboo and its fibers. *Bamboo-Current and Future Prospects*, *IntechOpen,* 145-164.
8. Abdul Khalil, H. P. S., Saurabh, C. K., Asniza, M., Tye, Y. Y., Fazita, M. R. N. et al. (2017). Nanofibrillated cellulose reinforcement in thermoset polymer composites. *Cellulose-Reinforced Nanofibre Composites*, *Woodhead Publishing,* 1-24.
9. Abdul Khalil, H. P. S., Saurabh, C. K., Syakir, M. I., Fazita, M. N., Bhat, A. et al. (2019). Barrier properties of biocomposites/hybrid films. *Mechanical and Physical Testing of Biocomposites, Fibre-Reinforced Composites and Hybrid Composites*, *Woodhead Publishing,* 241-258.
10. Ismail, H., Haw, F. S. (2008). Effects of palm ash loading and maleated natural rubber as a coupling agent on the properties of palm-ash-filled natural rubber composites. *Journal of Applied Polymer Science, 110(5),* 2867-2876.
11. Bhat, A. H., Abdul Khalil, H. P. S. (2011). Exploring "nano filler" based on oil palm ash in polypropylene composites. *BioResources, 6(2),* 1288-1297.
12. Ibrahim, M. S., Sapuan, S. M., Faieza, A. A. (2012). Mechanical and thermal properties of composites from unsaturated polyester filled with oil palm ash. *Journal of Mechanical Engineering and Sciences, 2,* 133-147.
13. Abdul Khalil, H. P. S., Fizree, H. M., Bhat, A. H., Jawaid, M., Abdullah, C. K. (2013). Development and characterization of epoxy nanocomposites based on nano-structured oil palm ash. *Composites Part B: Engineering, 53,* 324-333.
14. Khalid, N. H. A., Hussin, M. W., Mirza, J., Ariffin, N. F., Ismail, M. A. et al. (2016). Palm oil fuel ash as potential green micro-filler in polymer concrete. *Construction and Building Materials, 102(1),* 950-960.
15. Park, S., Baker, J., Himmel, M., Parilla, P., Johnson, D. (2010). Cellulose crystallinity index: measurement techniques and their impact on interpreting cellulase performance. *Biotechnology for Biofuels, 3(1),* 10.

16. Biener, J., Wittstock, A., Baumann, T. F., Weissmüller, J., Bäumer, M. et al. (2009). Surface chemistry in nanoscale materials. *Materials, 2(4),* 2404-2428.
17. Saurabh, C. K., Gupta, S., Bahadur, J., Mazumder, S., Variyar, P. S. et al. (2015). Mechanical and barrier properties of guar gum based nano-composite films. *Carbohydrate Polymers, 124,* 77-84.
18. Sipaut, C., Ahmad, N., Adnan, R., Rahman, I., Bakar, M. et al. (2007). Properties and morphology of bulk epoxy composites filled with modified fumedsilica-epoxy nanocomposites. *Journal of Applied Polymer Science, 7(1),* 27-34.
19. Williams, P. J., Biernacki, J. J., Rawn, C. J., Walker, L., Bai, J. (2005). Microanalytical and computational analysis of class F fly ash. *ACI Materials Journal, 102(5),* 330.
20. Chindaprasirt, P., Rukzon, S., Sirivivatnanon, V. (2008). Effect of carbon dioxide on chloride penetration and chloride ion diffusion coefficient of blended Portland cement mortar. *Construction and Building Materials, 22(8),* 1701-1707.
21. Tangchirapat, W., Saeting, T., Jaturapitakkul, C., Kiattikomol, K., Siripanichgorn, A. (2007). Use of waste ash from palm oil industry in concrete. *Waste Management, 27(1),* 81-88.
22. Abdul Khalil, H. P. S., Fizree, H. M., Jawaid, M., Alattas, O. S. (2011). Preparation and characterization of nano-structured materials from oil palm ash: a bio-agricultural waste from oil palm mill. *BioResources, 6(4),* 4537-4546.
23. Agarwal, B. D., Broutman, L. J., Chandrashekhara, K. (1990). *Analysis and performance of fiber composites*, pp. 1-30. John Wiley & Sons. Inc., New York.
24. Khoshnoud, P., Abu-Zahra, N. (2018). The effect of particle size of fly ash (FA) on the interfacial interaction and performance of PVC/FA composites. *Journal of Vinyl and Additive Technology, 25(2),* 134-143.
25. Fu, S. Y., Feng, X. Q., Lauke, B., Mai, Y. W. (2008). Effects of particle size, particle/matrix interface adhesion and particle loading on mechanical properties of particulate-polymer composites. *Composites Part B: Engineering, 39(6),* 933-961.
26. Nwanonenyi, S., Obidiegwu, M., Onuegbu, G. (2013). Effects of particle sizes, filler contents and compatibilization on the properties of linear low density polyethylene filled periwinkle shell powder. *International Journal of Engineering and Science, 2(2),* 1-8.
27. Pan, P., Liang, Z., Cao, A., Inoue, Y. (2009). Layered metal phosphonate reinforced poly(L-lactide) composites with a highly enhanced crystallization rate. *ACS Applied Materials & Interfaces, 1(2),* 402-411.
28. Khoshnoud, P. (2017). *Polymer foam/fly ash composites: evaluation of mechanical, interfacial, thermal, viscoelastic and microstructural properties (Ph.D. Thesis)*. University of Wisconsin-Milwaukee, United States.
29. Yu, X., Qu, X., Naito, K., Zhang, Q. (2011). Synthesis, tensile, and thermal properties of polyimide/diamond nanocomposites. *Journal of Reinforced Plastics and Composites, 30(8),* 661-670.